Aeronautical Research Institute, University of Tokyo
Report No. 332, June 1958

Analysis for Deep-Drawing of Cylindrical Shell based on Total Strain Theory and Some Formability Tests

By

Shinji FUKUI,
Hirozo YURI and Kiyota YOSHIDA*

Summary. An analysis, based on the total strain theory combined with octahedral shear theory, for the deep-drawing of cylindrical shell is developed in this paper. For this purpose the actual process is traced as exactly as possible, the local variations of thickness and strain hardening being taken into consideration. The calculated values for strain distributions and punch forces are compared with experimental results on quasi-isotoropic phosphor bronze sheets drawn by plane die and conical die. Good agreements are obtained. Furthermore, calculated values thus obtained are compared with results by approximate formulas which have been suggested already by other investigators. It is revealed that the strain distributions over the flange region are nearly independent of sheet materials.

Furthermore, according to results of investigations related to formability testing, it has been confirmed that the diameter of the flange at the point of fracture of blank having the the diameter exceeding its drawing limit, formed with a conical die can properly be used in comparing the formability qualities of materials.

INTRODUCTION

The deep-drawing process is a technical process in which a thin sheet of blank material is usually drawn through a solid die by a solid punch and deformed into a deep seamless cup.

The shape of the cup is determined by the form of the die and punch. This process is very convenient for mass production of vessels from thin sheet and is extensively used in the mechanical, automotics and aeronautical industries.

Many investigators have dealt with problems associated with axially symmetrical cylindrical cups or shells either theoretically or experimentally because these are fundamental and the simplest. M. Sommer [*1*], G. Sachs [*2*] and others [*3*] have calculated stress, strain distributions in these cups or shells and made comparisons with experimental findings. Except for Sachs however, many of the investigators neglected the factor of the components in the direction of the thickness who moreover treated both stress and strain as if they were two dimentional distribution. As the component of stress in the direction of thickness is small in comparison

* Scientific Research Institute, Ltd.

with other components, its neglection is considered permissable but not quite disregardable because of the factors of non-uniformity in the change of thickness, and substantial strains ranging from 20–40% according to many experiments. Consequently, an analysis with respect to the treatment of strain as a three dimensional distribution under plane stress is desirable to ascertain the actual phenomena more precisely.

One investigator [4] has proposed the equation of equilibrium of stress by consideration of the variation of thickness. A solution of the equation of equilibrium in the strain-hardening range based on the total strain or deformation theory [5] is dealt with in this paper. The relation between stress and strain in the plastic range is assumed to be governed by the shearing strain energy theory and the equivalent stress and strain correlated according to the power law. The distribution of stress and strain and the force acting on a punch are calculated and compared with experimental findings.

The finding of M.H. Lee Wu [6] evolved from studies on plane-plastic stress problems dealing with axially symmetrical objects such as a circular membrane under pressure, a rotating disk and an infinite plate with a circular hole and the procedure of the aforementioned Sachs are very useful for reference but insofar as treatise related to deep drawing is concerned, there is very little in the way of bibliography except for R. Hills [7] brief work founded on the flow theory.

In actual production work, the selection of materials of proper properties becomes very important, in order to gain optimum results through full utilization of the features offered by deep drawing work. Therefore, investigations were also made in respect to simple and practical formability testing.

Symbols

The following symbols are used in this paper.

$\varepsilon_1, \varepsilon_2, \varepsilon_3$; Principal logarithmic strains.

$\lambda_1, \lambda_2, \lambda_3$; Conventional strains in radial, thickness, and circumferential directions.

$\sigma_1, \sigma_2, \sigma_3$; Mean principal true stresses.

σ_{10}, σ_{30}; σ_1 and σ_3 at outside periphery.

L; Plastic coefficient, function of stress state.

$\bar{\sigma}$; Equivalent stress. $\{\sigma_1^2+\sigma_2^2+\sigma_3^2 -\sigma_1\sigma_2-\sigma_2\sigma_3-\sigma_3\sigma_1\}^{\frac{1}{2}}$

$\bar{\varepsilon}$; Equivalent logarithmic strain. $\left\{\frac{2}{3}(\varepsilon_1^2+\varepsilon_2^2+\varepsilon_3^2)\right\}^{\frac{1}{2}}$

σ_p; True tensile stress.

ε_p; Logarithmic tensile strain.

$\varepsilon_b, \varepsilon_t$; Logarithmic strains in breadth and thickness for simple tension.

n; Number of power, for power law.

K'; Coefficient for power law.

m, K; Coefficients related to n, K'.

r; Initial radial coordinate.

r_0; Initial outside radius.

R; Radial coordinate for derformed state.

R_0; Outside radius for derformed state.

T; Thickness of blank.

t_0; Initial thickness of blank.

H; Holding force.

u; Radial displacement.

r_d; Profile radius at shoulder of die.

R_d; $r_d+T/2$.
d_1; Diameter of punch.
r_p; Profile radius at top corner of punch.
d_2; Diameter of hole in die.
θ; Angle between axis of punch and face of die.
α; Angular coordinate.
δ; Angular clearance.

PART I
ANALYSIS FOR STATE OF STRESS AND STRAIN

1. *Stress-strain relation in plastic deformation*

The following stress-strain relations are obtained from the so-called total strain theory and shearing strain energy theory developed by Hencky, Nadai et al.

$$\left.\begin{aligned} L\varepsilon_1&=\left\{\sigma_1-\frac{1}{2}(\sigma_2+\sigma_3)\right\}\\ L\varepsilon_2&=\left\{\sigma_2-\frac{1}{2}(\sigma_3+\sigma_1)\right\}\\ L\varepsilon_3&=\left\{\sigma_3-\frac{1}{2}(\sigma_1+\sigma_2)\right\}\end{aligned}\right\}, \tag{1}$$

$$L\bar{\varepsilon}=\bar{\sigma}. \tag{2}$$

In the above, L is not a constant but a variable coefficient determined by the state of stress. Also $\bar{\varepsilon}$ and $\bar{\sigma}$ are correlated by the power law as follows.

$$\bar{\sigma}=K'(\bar{\varepsilon})^n. \tag{3}$$

Since $\bar{\sigma}$ and $\bar{\varepsilon}$ correspond to σ_p and ε_p respectively in simple tension, K', n are determined from simple tensile tests on the material under study.

Combining (1), (2) and (3), we have:

$$\left.\begin{aligned} \varepsilon_1&=K(\bar{\sigma})^m\left\{\sigma_1-\frac{1}{2}(\sigma_2+\sigma_3)\right\}=\left(\frac{1}{K'}\right)(\bar{\varepsilon})^{(1-n)}\left\{\sigma_1-\frac{1}{2}(\sigma_2+\sigma_3)\right\}\\ \varepsilon_2&=K(\bar{\sigma})^m\left\{\sigma_2-\frac{1}{2}(\sigma_3+\sigma_2)\right\}=\left(\frac{1}{K'}\right)(\bar{\varepsilon})^{(1-n)}\left\{\sigma_2-\frac{1}{2}(\sigma_3+\sigma_1)\right\}\\ \varepsilon_3&=K(\bar{\sigma})^m\left\{\sigma_3-\frac{1}{2}(\sigma_1+\sigma_2)\right\}=\left(\frac{1}{K'}\right)(\bar{\varepsilon})^{(1-n)}\left\{\sigma_3-\frac{1}{2}(\sigma_1+\sigma_2)\right\}\end{aligned}\right\}, \tag{4}$$

where

$$K=\left(\frac{1}{K'}\right)^{\frac{1}{n}},\qquad m=\frac{(1-n)}{n}.$$

2. *Equation of stress equilibrium and its solution in flange part A-B*

Referring to Fig. 1, the object under study for stress analysis can be devided into two parts i.e. the flange (A-B) which comes into contact with the face of the die and the part (B-C) which touches the shoulder of the die hole. The analysis for the general case of a conical die i.e., the generating line of die's face forming an angle θ with the central axis of a punch will be treated with hereinafter.

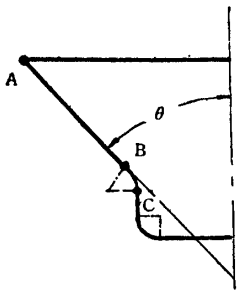

FIGURE 1. Configuration of blank at a certain stage of drawing process by conical die.

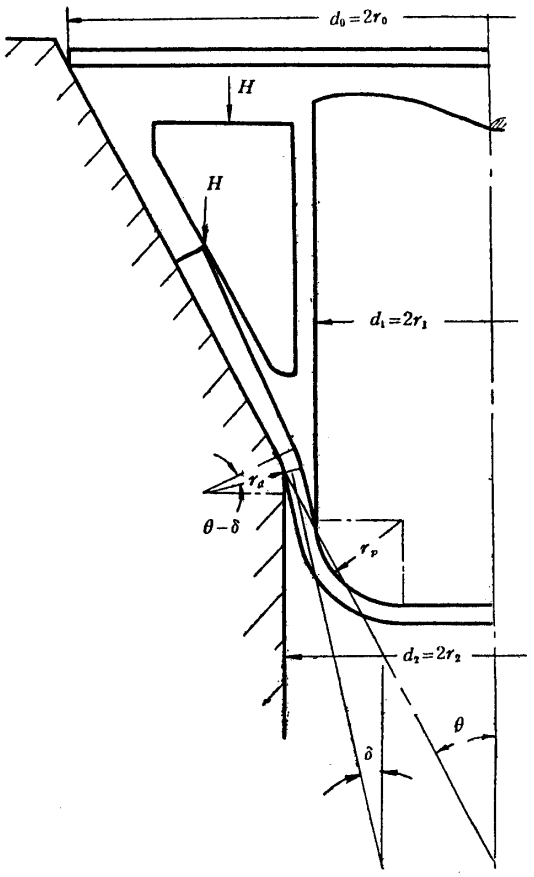

FIGURE 2. Manner of blank holding, and symbols for tool and blank dimensions.

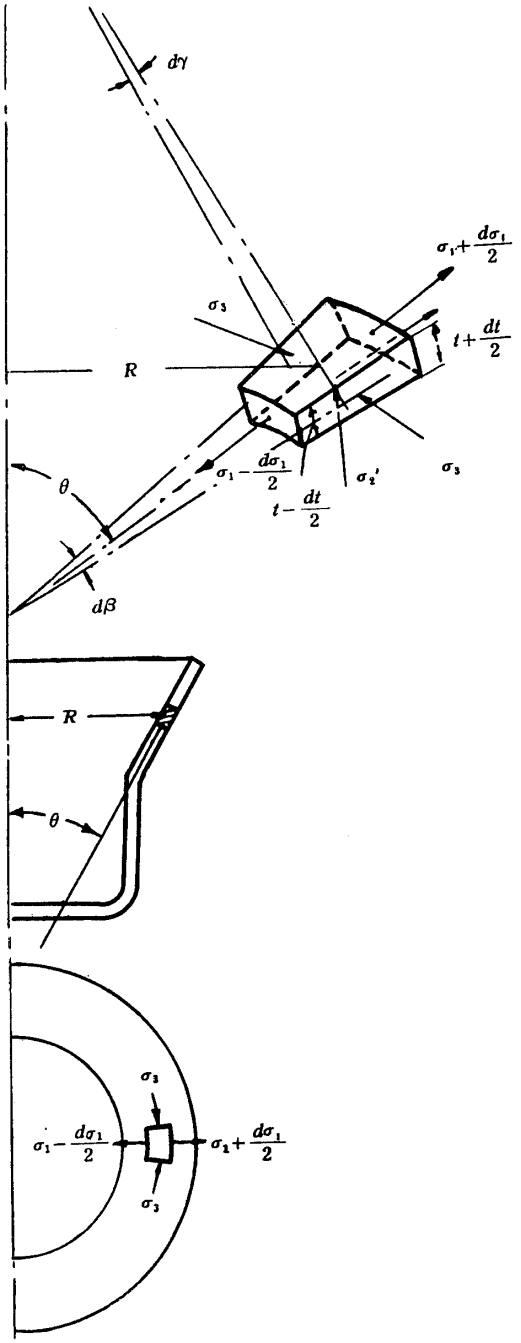

FIGURE 3. Acting stresses in faces of a sector element in part AB.

Now, as the thickness of the blank at the outer periphery is the greatest at the instant of deep drawing, the holding force H is assumed to act on the outer periphery as illustrated in Fig. 2 in accordance with Sachs method. Accordingly, the stress component in the direction of the thickness due to the holding force is small in the part other than the periphery and may thus be neglected. However, a contact stress σ_2' in the direction of thickness appears in the surface of the blank in contact with the die's face due to the circumferential compressive stress σ_3. De-

signating the radial, thickness and circumferential directions of the principal stress and strain by the numerals 1, 2 and 3 respectively, we have the equation for σ_2' as

$$\sigma_2'=\sigma_3 \cos\theta\left(\frac{T}{R}\right), \tag{5}$$

wherein T is the thickness and R is the radial coordinate measured from the axis of the punch to a predetermined point. The mean stress in the direction of thickness σ_2 due to σ_2' will be smaller than σ_2' given by (5) because, as noted before, no contact stress exists in the upper surface of the blank. Furthermore, the ratio (T/R) will be small when R is sufficiently large for a thin blank which makes σ_2 smaller than σ_1, σ_3 and σ_2 may be neglected.

The equation for equilibrium of stress in the flange part Fig. 3 is given as

$$\frac{d(\sigma_1\cdot R\cdot T)}{dR}=(1+\mu\cot\theta)\sigma_3\cdot T \tag{6}$$

in which the tensile stress is taken as positive.

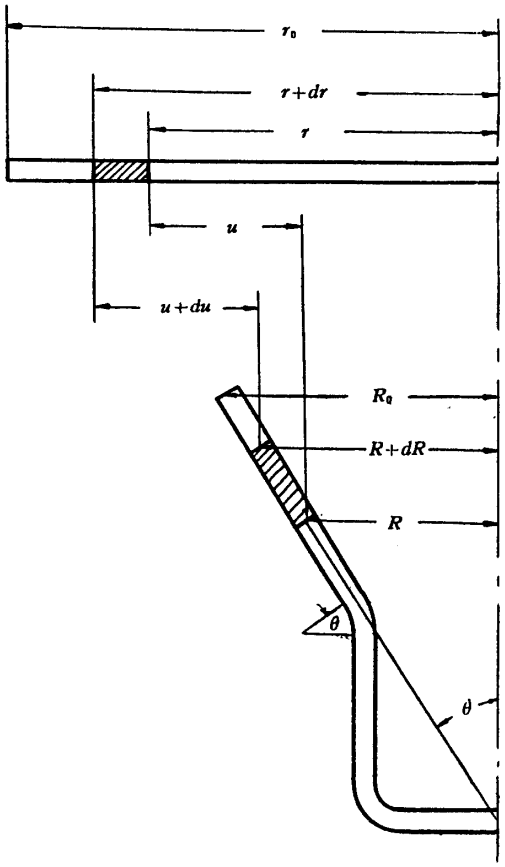

FIGURE 4. Displacement of an element in part AB.

The displacement of material in a blank is next considered. A part between r and $r+dr$ before deformation is assumed to displace to a position between R and $R+dR$ by working. Taking the amount of radial displacement of r as u, the displacement of $r+dr$ then becomes $u+du$. The conventional radial strain λ_1 and conventional circumferential strain λ_3 are than determined by the following equations

wherein u is taken as positive in the direction of increasing r.

$$\lambda_1=\frac{\dfrac{dr+du}{\sin\theta}-dr}{dr}=\frac{1}{\sin\theta}\frac{du}{dr}+\left(\frac{1}{\sin\theta}-1\right),$$

$$\lambda_3=\frac{u}{r},$$

$$\therefore\quad \frac{d\lambda_3}{dr}=\frac{1}{r}\left(\frac{du}{dr}-\frac{u}{r}\right)=\frac{1}{r}\{\sin\theta(1+\lambda_1)-(1+\lambda_3)\}. \tag{7}$$

Equation (7) may also be written as

$$e^{\varepsilon_3}\frac{d\varepsilon_3}{dr}=\frac{1}{r}(\sin\theta\, e^{\varepsilon_1}-e^{\varepsilon_3}), \tag{8}$$

according to the relations $(1+\lambda_1)=e^{\varepsilon_1}$, $(1+\lambda_3)=e^{\varepsilon_3}$ between logarithmic and conventional strains.

Now, the following equation for strain (9)

$$\frac{d\varepsilon_3}{dR}=\frac{1}{R}\left(1-\frac{1}{\sin\theta}e^{\varepsilon_3-\varepsilon_1}\right) \tag{9}$$

is obtained by using the following relations obtained by transforming the independent variabler r (initial radius before deformation) to R (radius after deforemation)

$$R=r+u,$$

$$\frac{d}{dr}=\frac{dR}{dr}\cdot\frac{d}{dR}=\left(\frac{du}{dr}+1\right)\frac{d}{dR}=(1+\lambda_1)\sin\theta\frac{d}{dR}=e^{\varepsilon_1}\sin\theta\frac{d}{dR}.$$

The distribution of stresses σ_1, σ_3 and strains ε_1, ε_2 and ε_3 are found by solving equations (6) and (9) simultaneously by utilizing the relations in (4). Equation (6) is first transformed as

$$R\frac{d\sigma_1}{dR}+R\sigma_1\frac{1}{T}\frac{dT}{dR}+\sigma_1=(1+\mu\cot\theta)\sigma_3, \tag{6'}$$

and $d\varepsilon_2/dR=(1/T)(dT/dR)$ from $\varepsilon_2=\ln(T/t_0)$, t_0 in the above represents the initial thickness of a blank before deformation.

Equation (6′) then becomes

$$R\frac{d\sigma_1}{dR}+R\sigma_1\frac{d\varepsilon_2}{dR}=(1+\mu\cot\theta)\sigma_3-\sigma_1. \tag{10}$$

Differentiating ε_2 in (4) by R, we obtain

$$\frac{d\varepsilon_2}{dR}=\frac{d\sigma_1}{dR}\left\{\frac{1}{4}Km(\bar{\sigma})^{m-2}(\sigma_1+\sigma_3)(\sigma_3-2\sigma_1)-\frac{1}{2}K(\bar{\sigma})^m\right\}$$
$$+\frac{d\sigma_3}{dR}\left\{\frac{1}{4}Km(\bar{\sigma})^{m-2}(\sigma_1+\sigma_3)(\sigma_1-2\sigma_3)-\frac{1}{2}K(\bar{\sigma})^m\right\}.$$

in which $\sigma_2=0$. Substituting the above in (10), we have

$$A\frac{d\sigma_1}{dR}+B\frac{d\sigma_3}{dR}=C. \tag{11}$$

In the above equations:

$$A=R+R\sigma_1\left\{\frac{1}{4}Km(\bar{\sigma})^{m-2}(\sigma_1+\sigma_3)(\sigma_3-2\sigma_1)-\frac{1}{2}K(\bar{\sigma})^m\right\},$$

$$B=R\sigma_1\left\{\frac{1}{4}Km(\bar{\sigma})^{m-2}(\sigma_1+\sigma_3)(\sigma_1-2\sigma_3)-\frac{1}{2}K(\bar{\sigma})^m\right\},$$

$$C=(1+\mu\cot\theta)\sigma_3-\sigma_1\,.$$

Furthermore, the equation:

$$\frac{d\varepsilon_3}{dR}=\frac{d\sigma_1}{dR}\left\{\frac{1}{4}Km(\bar{\sigma})^{m-2}(2\sigma_1-\sigma_3)(2\sigma_3-\sigma_1)-\frac{1}{2}K(\bar{\sigma})^m\right\}$$
$$+\frac{d\sigma_3}{dR}\left\{\frac{1}{4}Km(\bar{\sigma})^{m-2}(2\sigma_3-\sigma_1)^2-K(\bar{\sigma})^m\right\},$$

is obtained by differentiating ε_3 in (4). Combining this relations and (9), we obtain

$$A'\frac{d\sigma_1}{dR}+B'\frac{d\sigma_3}{dR}=C' \tag{12}$$

in which

$$A'=\frac{1}{4}Km(\bar{\sigma})^{m-2}(2\sigma_1-\sigma_3)(2\sigma_3-\sigma_1)-\frac{1}{2}K(\bar{\sigma})^m\,,$$

$$B'=\frac{1}{4}Km(\bar{\sigma})^{m-2}(2\sigma_3-\sigma_1)^2+K(\bar{\sigma})^m\,,$$

$$C'=\frac{1}{R}\left\{1-\frac{1}{\sin\theta}e^{\frac{3}{2}K(\bar{\sigma})^m(\sigma_3-\sigma_1)}\right\}.$$

The equations

$$\left.\begin{aligned}\frac{d\sigma_1}{dR}&=\frac{B'C-BC'}{AB'-A'B}\\ \frac{d\sigma_3}{dR}&=\frac{AC'-A'C}{AB'-A'B}\end{aligned}\right\}, \tag{13}$$

are obtained by solving simultaneous equations (11) and (12). As the right hand side in the equations (13) are functions of σ_1, σ_3 and R, (13) may be integrated numerically when the initial values of stresses σ_{10}, σ_{30} at the outer periphery are known. The values of initial stresses are considered in two cases in this presentation.

a) *Case for flat die under the action of a holding force H*

In this case, we will assume that the outside diameter $2R_0$, and holding force H is assumed to act as a concentrated force on R_0. σ_2 due to the force H is neglected but the radial frictional resistance due to the force H is taken as σ_{10} for $R=R_0$ in accordance with Sachs' consideration (1). We will then obtain the following equations:

$$\varepsilon_{30}=\ln\frac{R_0}{r_0}=K(\bar{\sigma})^m\left(\sigma_{30}-\frac{\sigma_{10}}{2}\right), \tag{14}$$

$$\sigma_{10}=\frac{2\mu H}{2\pi R_0T_0}=\frac{\mu H}{\pi R_0t_0}e^{K(\bar{\sigma})^m\left(\frac{\sigma_{10}+\sigma_{30}}{2}\right)}. \tag{15}$$

The initial values of σ_{10}, σ_{30} are found by solving the simultaneous equations (14), (15) graphically as shown in Fig. 5.

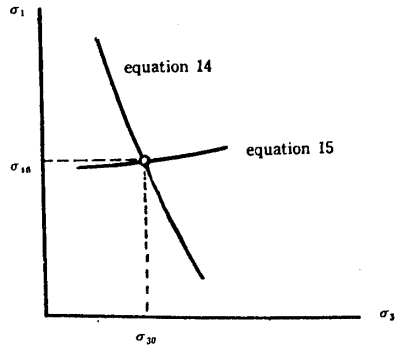

FIGURE 5. Graphical solutions of σ_{10}, σ_{30} for numerical integration.

b) *Case for conical die with no holding force*

A holding force is unnecessary for deep-drawing with a conical die when the ratio of r_0/t_0 is smaller than 25–35. Therefore, if $\sigma_{10}=0$ for $R=R_0$ is assumed in the case and the circumferential compression on the periphery is considered uniaxial, $\varepsilon_{30}=\ln(R_0/r_0)$ would be found from the following equation.

$$\sigma_{30}=K'\left(\ln\frac{R_0}{r_0}\right)^n. \tag{16}$$

3. *Equation of stress equilibrium and its solution in part B-C in contact with the die shoulder*

The equation of equilibrium in this part as derived by one investigaton [4] is given as follows:

$$\frac{d(\sigma_1\cdot R\cdot T)}{d\alpha}=-\sigma_3\cdot T\{\sin(\theta-\alpha)+\mu\cos(\theta-\alpha)\}R_d+\mu\sigma_1\cdot R\cdot T, \tag{17}$$

where $R_d=r_d+T/2$ and the angle θ, present the included angle between the axis of a punch and the slope of the flange. α represent the angle between a point B and preconsidered point on the die shoulder part, as illustrated in Fig. 6.

The equation of strain is given as

$$\frac{d\varepsilon_3}{dR}=\frac{1}{R}\left\{1-\frac{1}{\sin(\theta-\alpha)}e^{\varepsilon_3-\varepsilon_1}\right\},$$

because the part between R and $R+dR$ is considered to be in contact with the conical die at an angle of $(\theta-\alpha)$ as in Fig. 7. The independent variable R in the equation $R=R_4+R_d-R_d\cos(\theta-\alpha)$ is transformed as a function of α as followes:

$$\frac{d}{dR}=\frac{d\alpha}{dR}\frac{d}{d\alpha}=\frac{-1}{R_d\sin(\theta-\alpha)}\frac{d}{d\alpha},$$

wherefrom, we have

$$\frac{d\varepsilon_3}{d\alpha}=\frac{-R_d}{R}\{\sin(\theta-\alpha)-e^{\varepsilon_3-\varepsilon_1}\}, \tag{18}$$

wherein R_d is taken as a constant for simplicity.

Then the following simultaneous equations:

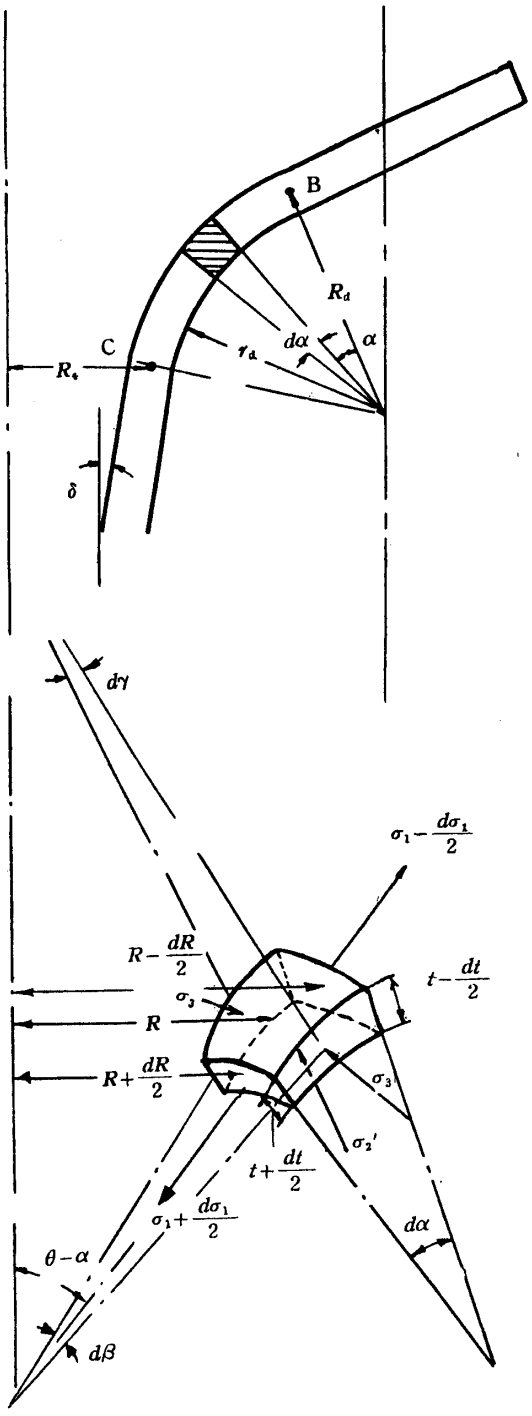

FIGURE 6. Acting stresses in faces of a sector element in part BC.

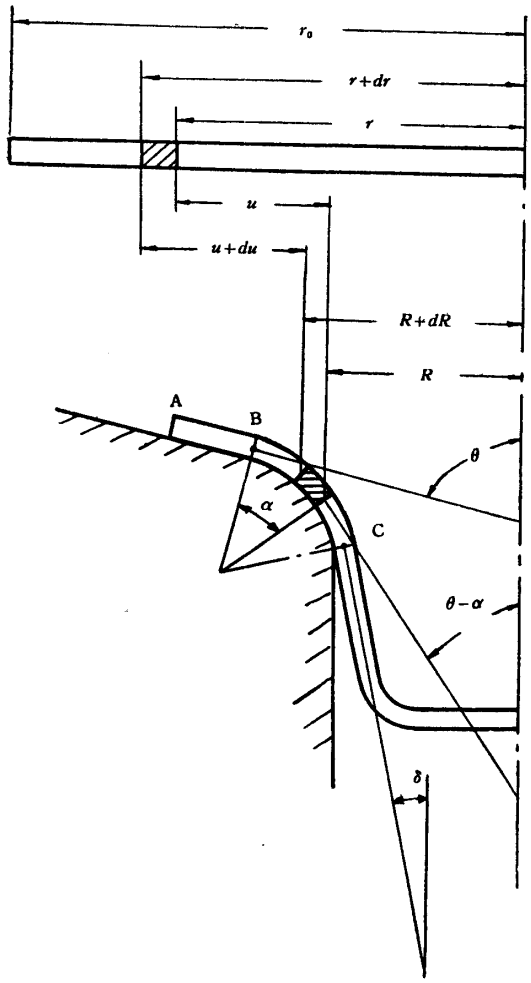

FIGURE 7. Displacement of an element in part BC.

$$\left.\begin{aligned}\frac{d\sigma_1}{d\alpha}&=\frac{B'C-BC'}{AB'-A'B},\\ \frac{d\sigma_3}{d\alpha}&=\frac{AC'-A'C}{AB'-A'B},\end{aligned}\right\} \tag{19}$$

are obtained from (18), (17) and (4) as before where

$$A=R+R\sigma_1\left\{\frac{1}{4}Km(\bar{\sigma})^{m-2}(\sigma_1+\sigma_3)(\sigma_3-2\sigma_1)-\frac{1}{2}K(\bar{\sigma})^m\right\},$$

$$B=R\sigma_1\left\{\frac{1}{4}Km(\bar{\sigma})^{m-2}(\sigma_1+\sigma_3)(\sigma_1-2\sigma_3)-\frac{1}{2}K(\bar{\sigma})^m\right\},$$

$$C=-\sigma_3\{\sin(\theta-\alpha)+\mu\cos(\theta-\alpha)\}R_d+\sigma_1\{\mu R+R_d\sin(\theta-\alpha)\},$$

$$A'=\frac{1}{4}Km(\bar{\sigma})^{m-2}(2\sigma_1-\sigma_3)(2\sigma_3-\sigma_1)-\frac{1}{2}K(\bar{\sigma})^m,$$

$$B'=\frac{1}{4}Km(\bar{\sigma})^{m-2}(2\sigma_3-\sigma_1)^2+K(\bar{\sigma})^m,$$

$$C'=-\frac{R_d}{R}\{\sin(\theta-\alpha)-e^{\frac{3}{2}K(\bar{\sigma})^m(\sigma_3-\sigma_1)}\},$$

$$R=R_4+R_d\{1-\cos(\theta-\alpha)\}.$$

The equations in (19) can be integrated numerically by using the initial values σ_1 and σ_3 found for the point B according to (13) in the preceding paragraph 2. The force P acting on the punch then can be calculated in accordance with the following equation

$$p={}_C\sigma_1\cdot t_0(1+{}_C\lambda_2)\cdot 2\pi R_4\cos\delta, \tag{20}$$

wherein ${}_C\sigma_1$ is stress and ${}_C\lambda_2$ is strain of thickness at the point C and δ is a clearance angle between the axis of the punch and a part below the point C as shown in Fig. 7.

4. *Solution when* $\bar{\varepsilon}=a+b\bar{\sigma}$

The stress-strain relations in the plastic range are given by the following equations.

$$\left.\begin{aligned}\varepsilon_1&=\frac{a+b\bar{\sigma}}{\bar{\sigma}}\left\{\sigma_1-\frac{1}{2}(\sigma_2+\sigma_3)\right\},\quad \varepsilon_2=\frac{a+b\bar{\sigma}}{\bar{\sigma}}\left\{\sigma_2-\frac{1}{2}(\sigma_1+\sigma_3)\right\},\\ \varepsilon_3&=\frac{a+b\bar{\sigma}}{\bar{\sigma}}\left\{\sigma_3-\frac{1}{2}(\sigma_1+\sigma_2)\right\}.\end{aligned}\right\} \tag{4'}$$

The solutions related to the flange part can be evolved similarly as noted in paragraph 2 from the simultaneous equations (13) and solving the equations (4'), (6) and (9). In these equations:

$$A=R+R\sigma_1\left\{\frac{a}{4(\bar{\sigma})^3}(\sigma_1+\sigma_3)(2\sigma_1-\sigma_3)-\frac{1}{2}\left(\frac{a}{\bar{\sigma}}+b\right)\right\},$$

$$B=R\sigma_1\left\{\frac{a}{4(\bar{\sigma})^3}(\sigma_1+\sigma_3)(2\sigma_3-\sigma_1)-\frac{1}{2}\left(\frac{a}{\bar{\sigma}}+b\right)\right\},$$

$$C=(1+\mu\cot\theta)\sigma_3-\sigma_1,$$

$$A'=\left\{\frac{a}{4(\bar{\sigma})^3}(2\sigma_1-\sigma_3)(\sigma_1-2\sigma_3)-\frac{1}{2}\left(\frac{a}{\bar{\sigma}}+b\right)\right\},$$

$$B'=\left\{\frac{-a}{4(\bar{\sigma})^3}(2\sigma_3-\sigma_1)^2+\left(\frac{a}{\bar{\sigma}}+b\right)\right\},$$

$$C'=\frac{1}{R}\left\{1-\frac{1}{\sin\theta}e^{\frac{3}{2}\left(\frac{a}{\bar{\sigma}}+b\right)(\sigma_3-\sigma_1)}\right\}.$$

Also, the solutions for the part B-C can be obtained from the simultaneous equations (19), solved by means of (4′), (17) and (18) similarly as in paragraph 3. Here, A, B, C, A', B', C' are given by the equations:

$$A=R+R\sigma_1\left\{\frac{a}{4(\bar{\sigma})^3}(\sigma_1+\sigma_3)(2\sigma_1-\sigma_3)-\frac{1}{2}\left(\frac{a}{\bar{\sigma}}+b\right)\right\},$$

$$B=R\sigma_1\left\{\frac{a}{4(\bar{\sigma})^3}(\sigma_1+\sigma_3)(2\sigma_3-\sigma_1)-\frac{1}{2}\left(\frac{a}{\bar{\sigma}}+b\right)\right\},$$

$$C=-\sigma_3\{\sin(\theta-\alpha)+\mu\cos(\theta-\alpha)\}R_d+\sigma_1\{\mu R+R_d\sin(\theta-\alpha)\},$$

$$A'=\left\{\frac{a}{4(\bar{\sigma})^3}(2\sigma_1-\sigma_3)(\sigma_1-2\sigma_3)-\frac{1}{2}\left(\frac{a}{\bar{\sigma}}+b\right)\right\},$$

$$B'=\left\{\frac{-a}{4(\bar{\sigma})^3}(2\sigma_3-\sigma_1)^2+\left(\frac{a}{\bar{\sigma}}+b\right)\right\},$$

$$C'=\frac{-R_d}{R}\left\{\sin(\theta-\alpha)-e^{\frac{3}{2}\left(\frac{a}{\bar{\sigma}}+b\right)(\sigma_3-\sigma_1)}\right\}.$$

The initial values for numerical integrations can be determined as before from (14) and (15) in paragraph 2.

5. *Approximate solution taking $\bar{\sigma}$ as constant throughout part but with consideration of the factor of change in thickness*

The general case of conical die having an angle θ is taken for illustrating the derivation of a solution according to an approximate method.

The variation of $\bar{\varepsilon}$ in the flange part is actually nominal when the deep drawing process proceeds moderately. For the purpose of illustration, the distribution of $\bar{\varepsilon}$ in the flange part is exemplified in Fig. 17, and the variation of $\bar{\sigma}$ for these $\bar{\varepsilon}$ may be small.

The solution given herein will provide fairly good results for the case involved wherein the stress component σ_2 in the direction of thickness is neglected.

Now, the equation for the stress component is given as

$$\bar{\sigma}=(\sigma_1^2+\sigma_3^2-\sigma_1\sigma_3)^{\frac{1}{2}}=k\,. \tag{21}$$

Which is assumed to be constant throughout the flange part for the stage of drawing involved.

The stress-strain relations in the plastic range are given by the following equation:

$$\varepsilon_1=Kk^m\left(\sigma_1-\frac{\sigma_3}{2}\right),\quad \varepsilon_2=Kk^m\left(-\frac{\sigma_1+\sigma_3}{2}\right),\quad \varepsilon_3=Kk^m\left(\sigma_3-\frac{\sigma_1}{2}\right). \tag{22}$$

Wherefore

$$\frac{d\varepsilon_2}{dR}=\frac{1}{T}\frac{dT}{dR}=-\frac{Kk^m}{2}\left(\frac{d\sigma_1}{dR}+\frac{d\sigma_3}{dR}\right).$$

Also from (21), we have the equations stress components as

$$\sigma_3=\frac{\sigma_1}{2}-\frac{1}{2}\sqrt{4k^2-3\sigma_1^2}\,.$$

$$\therefore \quad \frac{d\sigma_3}{dR}=\frac{1}{2}\frac{d\sigma_1}{dR}+\frac{\sqrt{3}}{2}\frac{\sigma_1}{\sqrt{\frac{4}{3}k^2-\sigma_1^2}}\frac{d\sigma_1}{dR}.$$

Combining the foregoing equations with the equation of equilibrium (6′), we derive the following equations.

$$\frac{1}{A\sigma_1+B\sqrt{C^2-\sigma_1^2}}\left[1-\frac{1}{4}Kk^m\left(3\sigma_1+\frac{\sqrt{3}\,\sigma_1^2}{\sqrt{C^2-\sigma_1^2}}\right)\right]d\sigma_1=-\frac{dR}{R}. \tag{23}$$

In the above:

$$A=\frac{(1+\mu\cot\theta)}{2},\quad B=\frac{(1+\mu\cot\theta)\sqrt{3}}{2},\quad C=\sqrt{\frac{4k^2}{3}}.$$

The second term in the bracket in equation (23) is introduced by taking the change in thickness into consideration. We can now find a solution for plane strain by neglecting this term whereby the comparison between plane strain and plane stress will be made easy.

Integrating equation (23), we have

$$\begin{aligned}&\frac{A}{2(A^2+B^2)}\ln(D^2-\sigma_1^2)-\frac{B}{A^2+B^2}\left\{\cos^{-1}\frac{\sigma_1}{C}+\frac{\sqrt{C^2-D^2}}{2D}\ln\frac{\alpha\cdot\gamma}{\beta\cdot\delta}\right\}\\&-\frac{1}{4}Kk^m\left[\frac{3A-\sqrt{3}B}{A^2+B^2}\sigma_1-\frac{3A-\sqrt{3}B}{2(A^2+B^2)}\cdot D\ln\frac{d+\sigma_1}{d-\sigma_1}-\frac{\sqrt{3}A+3B}{A^2+B^2}\sqrt{C^2-\sigma_1^2}\right.\\&\left.+\frac{1}{2}\left\{\frac{\sqrt{3}AD^2-3B(C^2-D^2)}{(A^2+B^2)\sqrt{C^2-D^2}}\right\}\ln\frac{\beta\cdot\gamma}{\alpha\cdot\delta}\right]=-\ln R+C',\end{aligned} \tag{24}$$

wherein:

$$D=\sqrt{\frac{B^2C^2}{A^2+B^2}},$$

$$\alpha=\sqrt{(C^2-D^2)(C^2-\sigma_1^2)}+(D+C)(C+\sigma_1),$$

$$\beta=-\sqrt{(C^2-D^2)(C^2-\sigma_1^2)}+(D+C)(C+\sigma_1),$$

$$\gamma=\sqrt{(C^2-D^2)(C^2-\sigma_1^2)}+(D-C)(C+\sigma_1),$$

$$\delta=\sqrt{(C^2-D^2)(C^2-\sigma_1^2)}-(D-C)(C+\sigma_1),$$

and C' is an integration constant determined by boundary conditions.

The first and second terms in equation (24) are the solutions for plane strain and the third term in square brackets is a correction term introduced by the factor of change in thickness. The question now arises as to the determination of a moderate value for k for evaluation of equation (24). It is of course desirable to have a mean value of $\bar{\sigma}$ over the flange part but is difficult of estimation wherefore k can only be taken as the value of $\bar{\sigma}$ at the outside periphery. Therefore, if the circumferential compression at the periphery is considered as pure compression for the conical die with no holding force, $\sigma_1=0$ wherefrom we will have $k=K'|(\ln R_0/r_0)^n|$.

Similarly as in the preceding approach, the equations representing the relation in part B-C is evolved as follows:

$$\frac{d\sigma_1}{d\alpha}=\frac{\sigma_1\{\mu R+R_d\sin(\theta-\alpha)\}-\{\sin(\theta-\alpha)+\mu\cos(\theta-\alpha)\}R_d\left\{\frac{\sigma_1}{2}-\frac{1}{2}\sqrt{4k^2-3\sigma_1^2}\right\}}{R\left\{1-\frac{3}{4}\sigma_1 Kk^m-\frac{3}{4}\sigma_1^2 Kk^m\frac{1}{\sqrt{4k^2-3\sigma_1^2}}\right\}}. \tag{25}$$

6. *Approximate solution according to maximum shearing stress theory assuming thickness and maximum shearing stress as being constant*

The approximate solution in this section is given for comparison with the foregoing solution.

The equation of equilibrium is simplified as

$$\frac{d(\sigma_1\cdot R)}{dR}=(1+\mu\cot\theta)\sigma_3\,. \tag{26}$$

Putting $\sigma_1-\sigma_3=2\tau=k$, Equation (26) is transformed to read as

$$\frac{d\sigma_1}{\mu\cot\theta\sigma_1-(1+\mu\cot\theta)k}=\frac{dR}{R}\,.$$

Integration the above, we will have

$$\sigma_1=C_1R^{\mu\cot\theta}+\frac{1+\mu\cot\theta}{\mu\cot\theta}k\,, \tag{27}$$

in which C_1 is an integration constant determined by boundary conditions and as in the preceding case, k taken as pure compressive stress σ_3 at the outside periphery for the conical die with no holding force i.e.,

$$k=|\sigma_3|=K'\left|\left(\ln\frac{R_0}{r_0}\right)^n\right|.$$

It is permissable to derive a solution for the part B-C by integrating to R and multiplying by $e^{\mu(\theta-\alpha)}$ to correct for frictional effect similarly as in accordance with Sachs' method.

Part II
Experimental and Calculated Results

Experiments on a flat die and conical die were undertaken in order to confirm the analysis stated in Part I. Measurements of strain distributions and drawing forces were compared against calculated values and the difference by calculation of the strain distributions in a variety of materials was checked, and values derived from approximate solutions related to drawing force were compared also.

1. *Experiment apparatus and materials*

The dimensional specifications of the flat die and conical die used in the experiments are given in Table 1. A blank holder was not employed with the conical die whereas a blank holding force of 300 kg was applied in drawing with a flat die.

TABLE 1. PUNCH AND DIE FOR EXPERIMENT

	Punch		Die	
	d_1 mm	r_p mm	d_2 mm	r_d mm
Flat die	30.0	6.0	31.5	3.0
Conical die	12.7	3.0	14.7	3.0

TABLE 2. MECHANICAL PROPERTIES OF PHOSPHOR BRONZE (Sn 7.5%, P 0.2%)

Ultimate strength σ_b kg/mm²	0.2% yield stress σ_s kg/mm²	Percentage elongation %	Hardness V.H.N.	Drawing limit $(d_1/d_0)_{\lim}$	Degree of directionality $*h_m/(d_0-d_2)$
39.1	10.8	79.0	81.2	0.397	0.02

* h_m ; Mean hight of ears.

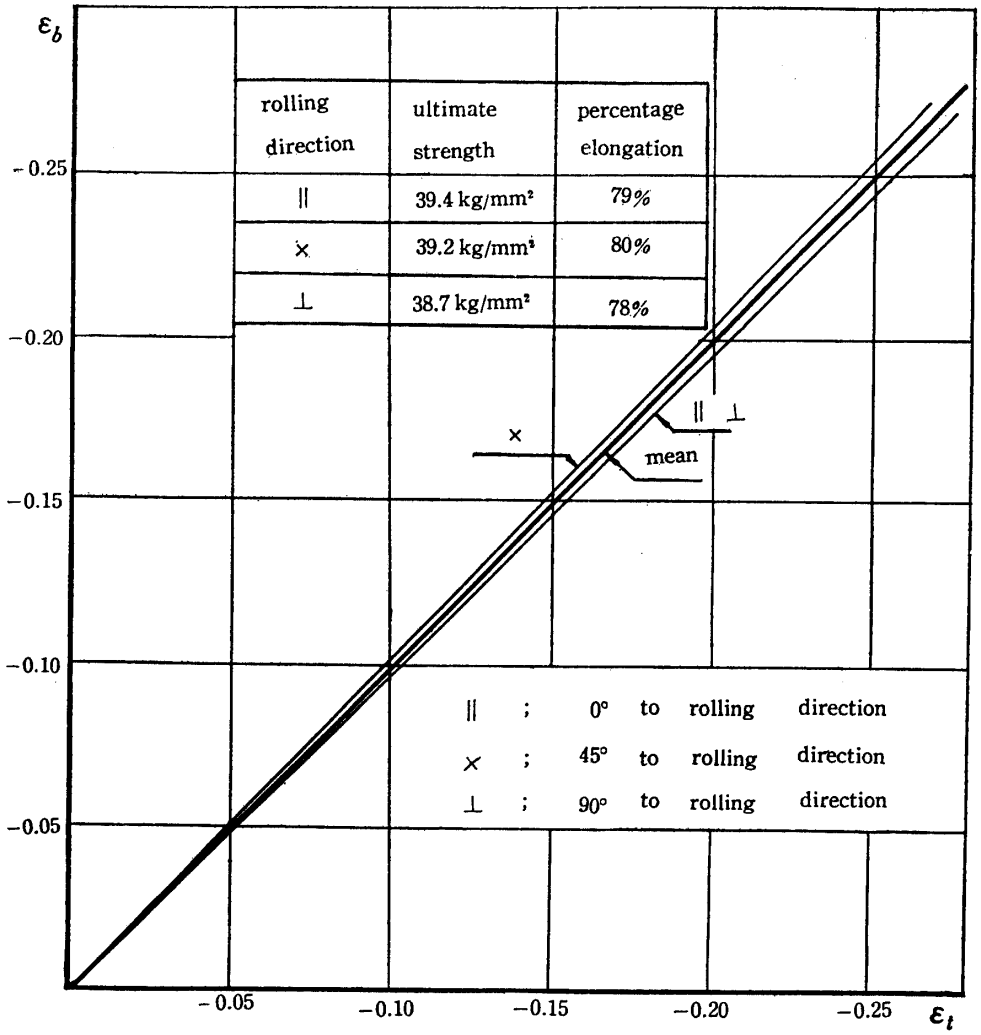

FIGURE 8. Relation between strains in width and thickness dimension of phosphor bronze testpiece under tension, and differences of ultimate strengths and percentage elongations are shown.

As for material for testing, extreme care was taken in selecting from among the materials available to the laboratory, rolled phosphor bronze sheet metals with the least directional deficienty. Plates about 0.52 mm in thickness and containing 7.5% Sn and 0.2% P were cut out into circular blanks of 60mm diameter and 31mm diameter for the flat die and conical die respectively and each annealed for 1 hour at 550°C. The mechanical properties of the annealed metal are given in Table 2. Among the properties (mechanical) given, the value of directionality for the selected material, though subject to question, was estimated according to the degree of directionality which could be attained through the measurement of the height of the ears on a drawn shell. This value was found to be 0.02 for the material concerned which is actually considered small.

The physical properties of the material i. e., tensile strength and percentage elongation as will as the difference in strains relative to the direction of width and thickness under tensile loading are also given for reference.

Tensile tests were also made on test pieces prepared by taking pieces paralled to, at 45 and 90 to the direction of rolling of the material and heat treated similarly as the blank material.

Fig. 8 shows the relations of strains in width and thickness. It will be noted in the figure that the strains in both cases are about equal within the limits of experimental error. The ultimate strength and percentage elongation in three directions are likewise found to be almost equal. Accordingly, the phosphor bronze material used in this experiment actually possessed very little directionality.

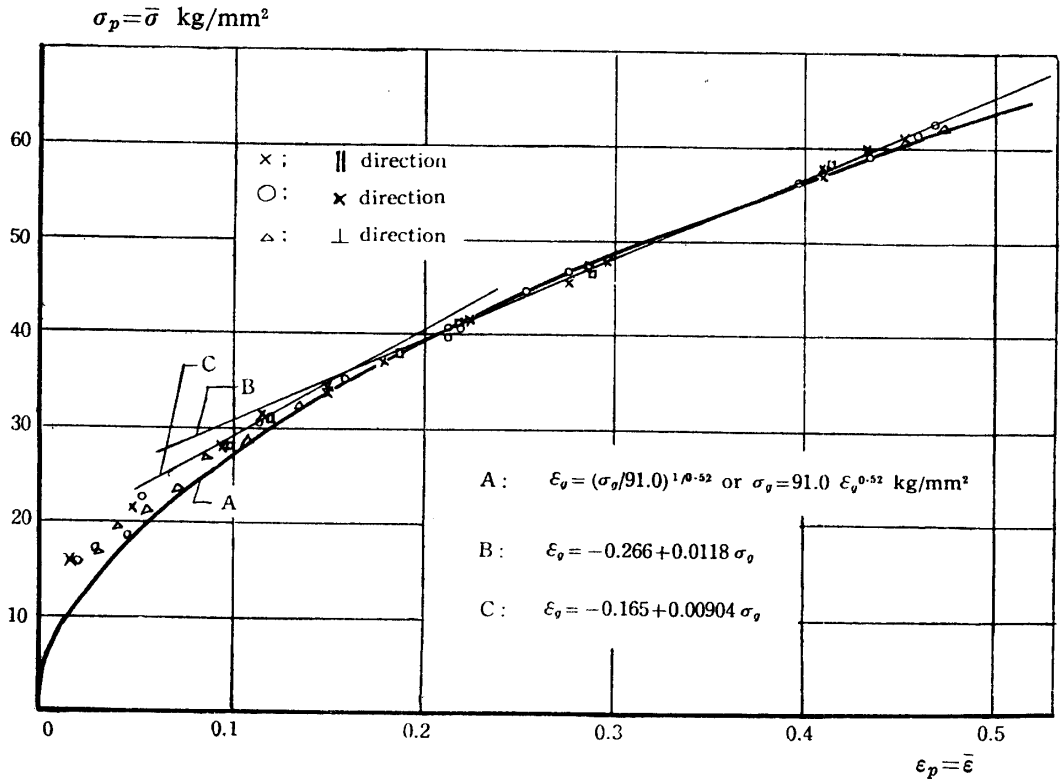

FIGURE 9. Plastic curve of phosphor bronze in tensile test. ($\sigma_g=\bar{\sigma}$, $\varepsilon_g=\bar{\varepsilon}$)

Fig. 9 indicates the relation between stress σ_p and strain ε_p i.e., $\bar{\sigma}$ versus $\bar{\varepsilon}$ obtained from tensile tests on three different directional pieces which when approximated according to the power low yields:

$$\bar{\sigma}=91.0(\bar{\varepsilon})^{0.52}\ \text{kg/mm}^2\,.$$

This is depicted by the solid line in the figure. When the strain is greater than 0.1, the experimental points fall on the curve very satisfactorily. Since the range of strains considered in this study are greater than 0.1, the approximate formula is deemed quite accurate.

Strain distributions in the flange portion was determined as follows. The top and bottom sides of an unworked blank was marked off accurately in 1mm intervals on the diameter drawn parallel to, at 45 and 90 to the direction of the material rolling.

After drawing the blank to a predetermined depth, the drawn piece was removed and measurements taken to determine the circumferential strain according to the undergiven equation through the change in diameter of the corresponding marks as shown in Fig. 10.

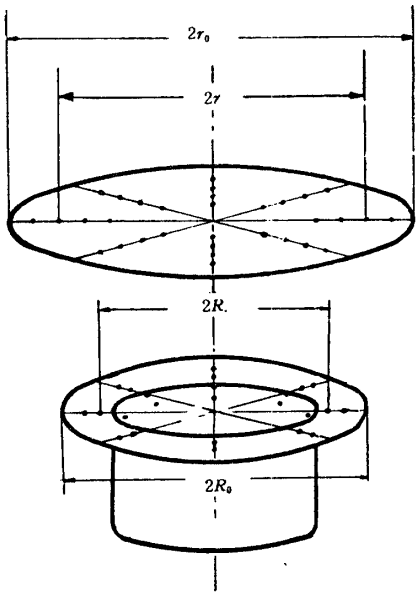

FIGURE 10. Measuring method of circumferential strain.

$$\lambda_3=\frac{R-r}{r}\,.$$

Measurements were next taken of the thickness at the midpoint between marks with an optimeter and the average of every other two measurements taken as the thickness at the point measured. If the thickness is denoted by T, the equation for strain is

$$\lambda_2=\frac{T-t_0}{t_0}\,,$$

in which t_0 refers to the thickness in the unworked material or blank. Strain along

the radius was calculated with the assumption of constancy in volume or in accordance with the following equation.

$$\lambda_1=\frac{1}{(1+\lambda_2)(1+\lambda_3)}-1\,.$$

2. *Experiment and calculation related to flat die*

A blank 60 mm in diameter and 0.52 mm in thickness was drawn with a flat die and as shown in Table 1. The stroke to produce the maximum drawing force was found to be about 17 mm. The drawing forces and corresponding strokes up to this maximum drawing force was investigated. The experimental findings related to drawing forces and strokes are shown tabulated in the following table.

Strokes of draw mm	Drawing forces kg	r_0 mm	t_0 mm	R_0 mm	ε_{30}
17.0	1,700	29.95	0.515	23.13	−0.258
11.0	1,480	29.95	0.515	26.63	−0.115

In the calculation for stress, the coefficient of friction between the blank and dieface is taken as $\mu=0.14$ according to experience. The initial values of stresses as determined from Eq. 14 and 15 are tabulated below.

Strokes of draw mm	σ_{10} kg/mm²	σ_{30} kg/mm²
17.0	0.99	−44.5
11.0	0.92	−29.5

The stress distribution shown plotted in Fig. 11 was found in accordance by numerical integration and by the use of the aforenoted initial values of stresses. Since a flat die is used, $\theta=\pi/2$.

The strain distribution can now be determined by employing the stress distribution values as determined above and by Eq. 4. The notations ○, △, ● in Fig. 12 denote the reference points ε_1, ε_2, ε_3 respectively: calculated values are shown by the solid line. Moreover, the values corresponding to the strokes shown good agreement. At this point, it should be pointed out that the actual thickness adjacent to the flange center and the portion in contact with the die shoulder is less than the calculated value because of the assumption of the blank holding force acting only around the periphery of the flange portion and zero stress ($\sigma_2=0$) over the remaining body and for the neglection of the effect of bending in the part in contact with the radius of the die shoulder.

Thus the radius R_4 and the radial stress $(\sigma_1)_{R=R_4}$ and the thickness $(T)_{R=R_4}$ at the point R_4 can be found through the values of stress and strain distributions.

If the angle between the drawn part and the axis of the punch is deduced graphically, the drawing force may then be calculated in accordance with Eq. 20.

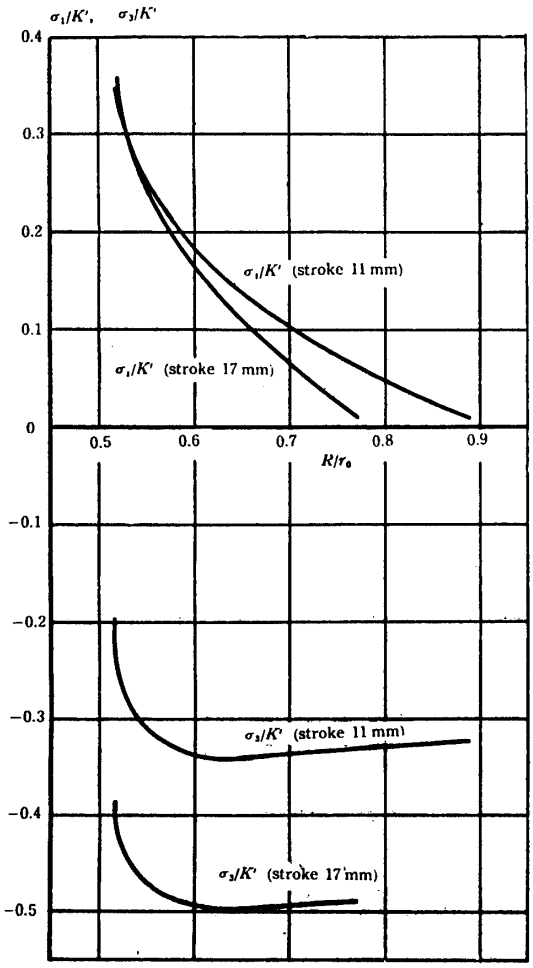

FIGURE. 11. Stress distributions over flange part AC, when drawn by flat die.

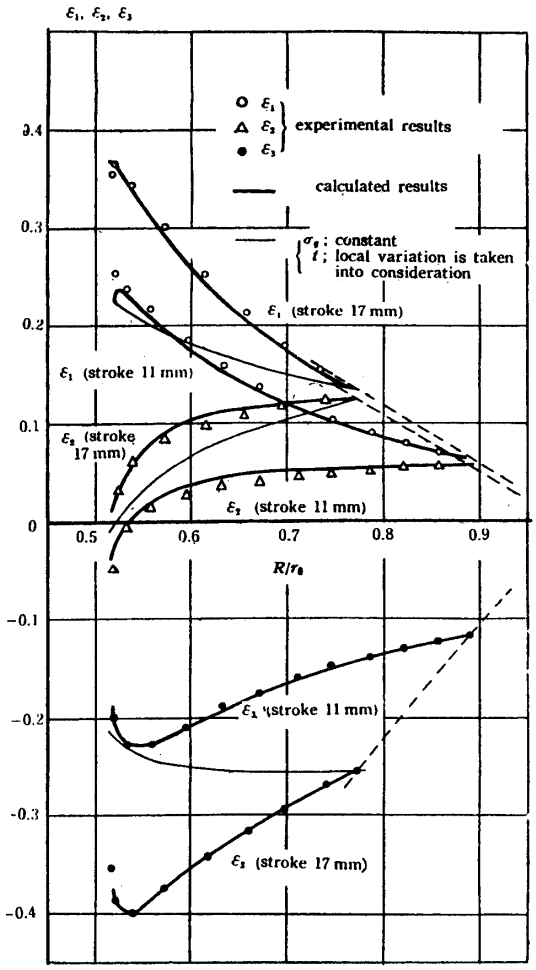

FIGURE 12. Strain distributions over flange part AC, when drawn by flat die.

Strokes of draw mm	Drawing forces (experimental values) kg	$(\sigma_1)_{R=R_4}$ kg/mm	$(T)_{R=R_4}$ mm	$\delta°$	R_4 mm	Drawing forces (calculated values) kg
17.0	1,700	32.45	0.525	0	15.46	1,655
11.0	1,480	30.36	0.505	7	15.49	1,482

Drawing forces are also found to agree roughly within the limits of allowable errors.

Now, and according to comparison of values strain distributions and drawing forces derived through experiments and calculations respectively, the conclusion is reached that the assumptions made in this analysis are fairly correct.

3. *Calculations and experiments related conical die*

In the experiments for deep drawing with a conical die, the maximum drawing force was reached when the punch was introduced 23 mm. Similarly as in the case with a flat die, the strain distributions corresponding to the stroke of the punch requiring the maximum drawing force and at a depth just immediate to the stroke of

maximum drawing force was measured. The tabulation below shows the drawing ing forces and other incidental values obtained through the experiment.

Strokes of draw mm	Drawing forces kg	r_0 mm	t_0 mm	R_0 mm	ε_{30}
23	855	15.5	0.515	9.97	−0.442
19	689	15.5	0.515	11.23	−0.323

A friction coefficient $\mu=0.14$ was used in the calculations similarly as with the case of the flat die. The initial values corresponding to the two strokes concerned are shown in the following table.

Strokes of draw mm	σ_{10} kg/mm	σ_{30} kg/mm
23	0	−59.52
19	0	−50.48

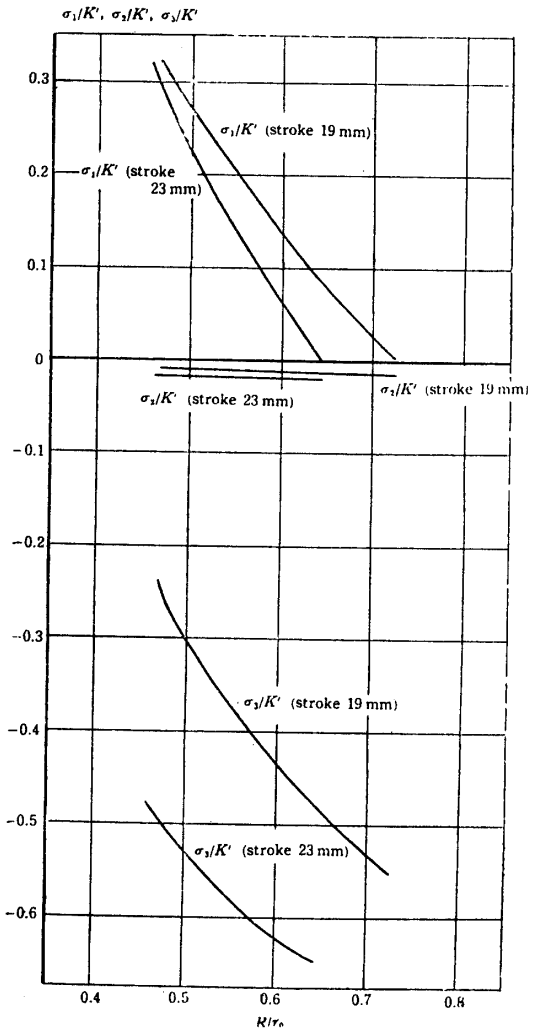

FIGURE 13. Stress distributions over flange part AC, when drawn by conical die.

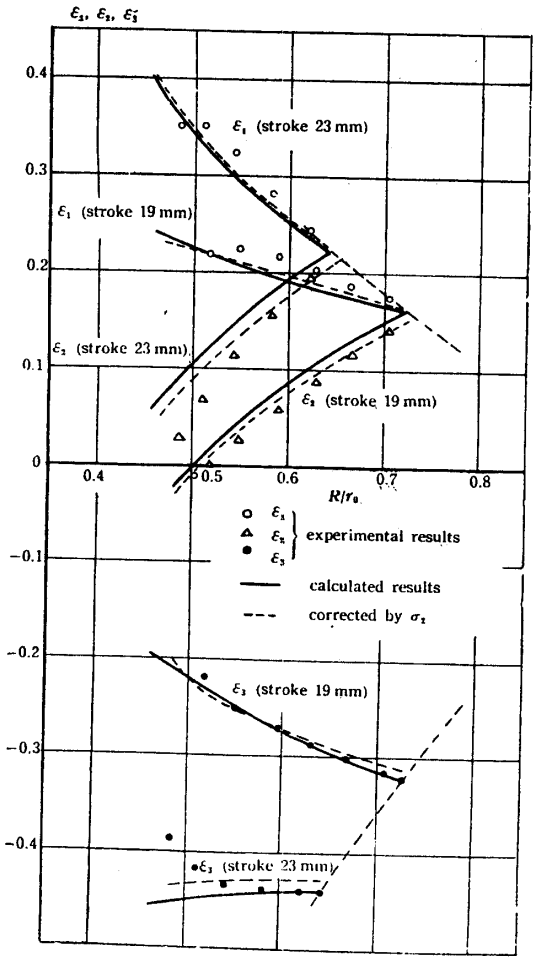

FIGURE 14. Strain distributions over flange part AC, when drawn by conical die.

Using the above noted initial values, the stress distributions found in accordance with the method of numerical integration are shown in Fig. 13. σ_2 in Fig. 13 is described subsequently.

The strain distributions as calculated from the aforenoted stress distributions and Eq. 4 are shown by the solid line in Fig. 14 in which, the marks ○, △, ● refer to points ε_1, ε_2, ε_3 respectively found by experiments.

Now, by employing the results found from calculations, R_4, $(\sigma_1)_{R=R_4}$ and $(T)_{R=R_4}$ are determined. If the value of δ is decided as in the case for the flat die, the drawing force may then be calculated in accordance with Eq. 20.

The clearance angle between the punch and die corresponding to a stroke of 19 mm is found to be rather large for the reason that the punch is introduced in to die hole only slightly. Accordingly, the angle of inclination between a point on the punch nose and the shoulder of the die is large but the effect of the shear forces becomes a problem.

Therefore, and in view of the meaninglessness of calculating the punch force for purpose of comparison, calculations were made for the case involving a stroke of 23 mm.

Stroke of draw mm	Drawing force (experimental value) kg	$(\sigma_1)_{R=R_4}$ kg/mm²	$(T)_{R=R_4}$ mm	$\delta°$	R_4 mm	Drawing force (calculated value) kg
23	855	29.4	0.561	6	7.1	757

The difference in strain distributions as compared to that in the flat die is relatively great. Moreover, the drawing force is found to be lower than the experimental values by about 12%. The causes for these differences are considered to be due to the following factors.

First, in establishing the initial values to be used in calculations, the blank in the course of working was removed from the conical die and measurements taken on its periphery. In the case of a conical die however, the effect of spring back is great. Consequently, the ε_3 adopted in establishing the initial value may differ from that under actual working conditions. Consequently, the strain distribution at the point R nearest the shoulder of the die should not be subject to comparison.

Furthermore, the blank places in a horizontal plane before it touches the wall of the conical die does not assume its conical shape by the circumferential strain alone but also simultaneously by the bending work. Consequently, the work hardening may actually be greater than as taken.

The above are considered as the principal causes and whereof, we find such a considerable difference between calculated and experimental values as compared that to for a flat die.

Now, insofar as the strain distribution is concerned, it is found that the value of ε_1 according to calculation is smaller than found by experiments whereas on the other hand, ε_2 by calculation is found to be greater. The difference in either case

is practically equal. Now, the cause for this difference is deemed to be due to the neglection of σ_2 previously noted and will therefore attempt to make a correction as a function of σ_2. Then, we will assume simply that applied from the die surface to the blank will be expressed by the following equation.

$$\sigma_2=\frac{T}{2R}\cos\theta\cdot\sigma_3 \quad \text{kg/mm}^2 .$$

By substituting the values of T for various strains on the basis of ε_2 heretofore determined, the values of σ_2 found therefore are shown plotted in Fig. 13. The strain distribution as corrected by placing the aforesaid distributions σ_2 and σ_1 and σ_3 by calculation in Eq. 5 is shown by the chain line in Fig. 14. From an overall viewpoint, it will be seen that a correction made with σ_2 will make the calculated values match the experimental values.

4. *Calculation for* $\bar{\varepsilon}=a+b\bar{\sigma}$ *(Chapter 1–4)*

It is well and fine if the relation $\bar{\sigma}\sim\bar{\varepsilon}$ found from tests can be sufficiently approximated to a given straight line. In this case however, it will be necessary to

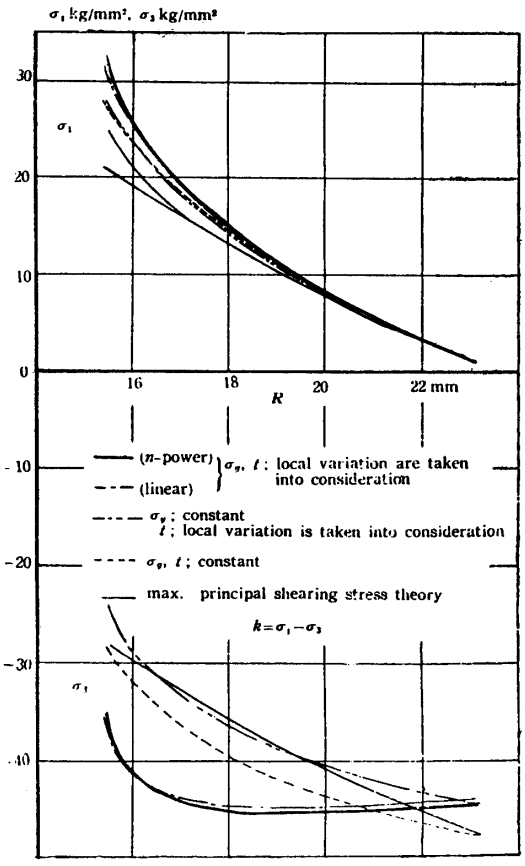

FIGURE 15. Stress distributions calculated by various method over flange part AC, when drawn to a stroke of 17mm by flat die. ($\sigma_\theta=\bar{\sigma}$).

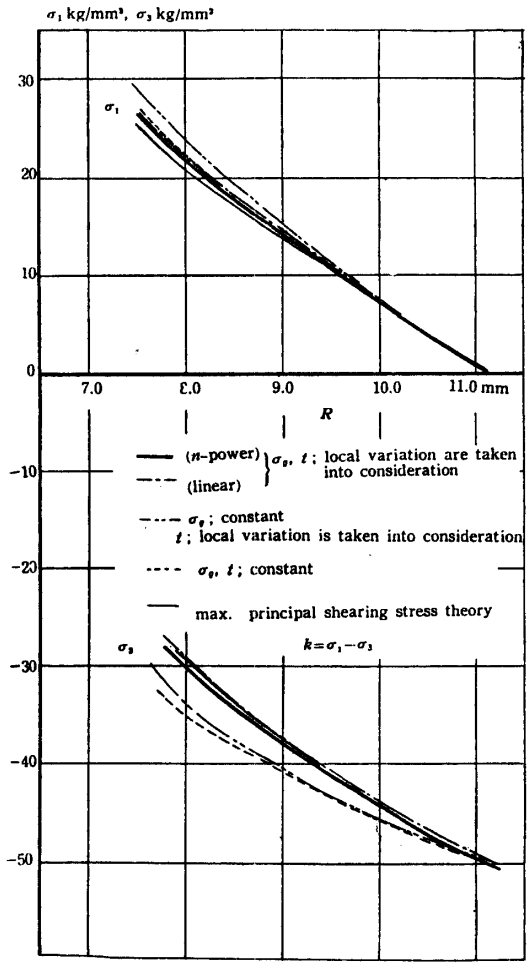

FIGURE 16. Stress distributions calculated by various method over flange part AC, when drawn to a stroke of 19mm by conical die. ($\sigma_\theta=\bar{\sigma}$).

change the values of the constants a and b depending on the degree of strain in the range in which calculations are to be made, if accuracy in calculated values are to be expected. If the $\bar{\sigma}\sim\bar{\varepsilon}$ is approximated by the power law, it will be found that the relation will approach a straight line for large values of $\bar{\varepsilon}$ while at the same time, the difference between $\bar{\sigma}=K'(\bar{\varepsilon})^n$ and $\bar{\varepsilon}=a+b\bar{\sigma}$ will diminish.

Taking for example the material subjected to experiments, the equation $\bar{\varepsilon}=-0.165+0.00904\bar{\sigma}$ will hold for $\bar{\varepsilon}$ within a range of values between 0.1~0.2. Above this strain range however, it was possible to make a sufficient approximation with $\bar{\varepsilon}=-0.266+0.0118\bar{\sigma}$ (Refer to Fig. 9). The stress distribution determined by utilization of the aforesaid relation in the case of deep drawing with a stroke of 17 mm with a flat die is shown by the single chain line in Fig. 15.

The above stress distribution when approximated according to the power law as shown by the solid line revealed practical coincidence except for a slight deviation below the decimal place. Strain distribution calculations were also made but both calculations were found to match at least to the extent that differences could not be distinguished graphically.

The single chain line shown in Fig. 16 indicates the calculated stress distribution for the case of deep drawing by means of a conical die employing a stroke of 19 mm. The differential in this case was also found to be extremely small.

The drawing force as indicated in the following was found in accordance with the method of calculation as described in Chapter 3. The deviation of this drawing force as determined by the power law was found to be within a few percent.

Drawing tools	Strokes of draw mm	Drawing forces kg		
		Experimental values	Calculated values (liner)	Calculated values (n power)
Flat die	17.0	1,700	1,566	1,655
	11.0	1,480	1,497	1,482
Conical die	23.0	855	770	757

5. *Comparison of various approximate solutions*

a) *Case involving thickness variation with assumption of non-variance of $\bar{\sigma}$ depending on location*

The selection of the $\bar{\sigma}$ to take as noted before poses a problem in proceeding with calculations. It would be desirable to use an average value between the extreme periphery and R_4 but unfortunately, $\bar{\sigma}$ at R_4 is unknown. For convenience therefore we assume that the $\bar{\sigma}$ at the peripheral edge is uniformly distributed the entire flange area so that in the case of flat die, it will permit calculation of σ_{10}, σ_{30} from Eq. 14 and Eq. 15 and derivation of $\bar{\sigma}$. In the case of a conical die, $\bar{\sigma}$ may be determined directly from a given circumferential strain.

For the purpose of illustration, an example is taken of employing a flat die involving a stroke of 17 mm. In this case, $\bar{\sigma}$ will be 45.01 kg/mm^2 and the stress distribution as determined from Eqs. 24, 25 will be depicted as shown by the double chain line in Fig. 15. The distribution of σ_3, with due consideration to the σ_3

resulting from the degree of work hardening in locations as found in Chapter 2 will vary greatly. However, the degree of deviation of σ_1 is only about 10%. On the other hand, the distribution of strain as shown by the fine line in Fig. 12 will involve a great variation. Consequently, and as both of the above differences will combine when solving for the drawing force, the force when compared to that determined by a strict solution will differ substantially from the experimental values. The drawing force determined by this approximate calculation is 1,391kg which is lower than the experimental value by approximately 18%.

The double chain line in Fig. 16 represents the calculation example for a conical die involving a stroke of 19mm. In this case, however, $\bar{\varepsilon}$ and $\bar{\sigma}$ were assumed as straight line functions. Similarly, as in the case for the flat die, the change in σ_1 as compared to the difference in σ_3 is small. However, σ_1 and σ_3 determined in accordance with the method of approximate calculation as compared to σ_1 and σ_3 found by strict solution will be found to be small in a flat die and large in a conical die. This phenomenon as indicated in Fig. 17 and for the stroke concerned in the calculation example is caused by the fact that whereas $\bar{\sigma}$ in the case of flat die will tend to increase with a decrease in R, it will became smaller in the case of a conical die involving the stroke of 19mm.

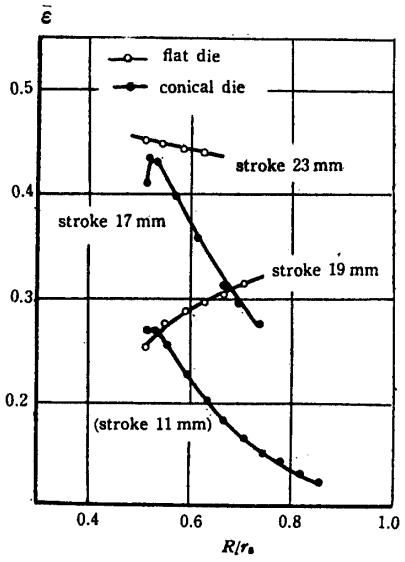

FIGURE 17. Distributions of ($\bar{\varepsilon}$) over flange part AC, when drawn by flat die and conical die.

b) *Case for neglection of both thickness variation and $\bar{\sigma}$ variation regardless of location (Chapter 1–5)*

The calculation examples covered herein apply to the case of a flat die with a stroke of 17mm and a conical die involving a stroke of 19mm.

In the calculation respect to the flat die, $\bar{\sigma}$ at the extreme pheriphery was solved by assuming two dimentional deformation of the blank and σ_{10} determined in accordance with the following equation. The assumption is also made that $\bar{\sigma}$ is evenly distributed over the range covered by the calculation.

$$\sigma_{10}=\frac{\mu H}{\pi R_0 t_0} \quad \mathrm{kg/mm^2}\,.$$

The stress distribution as determined from Eqs. 24, 25 with the preclusion of the corrective factor related to thickness variation is shown by the chain line in Fig. 15. It will be noted also in this case that the variation of σ_3 is substantial whereas, the the difference in σ_1 is small and moreover shown very little difference from the results in (a). The drawing force of 1,389 kg by calculation differs from that in (a) by only 2 kgs and is approximatery 18% lower than the experimental value.

The calculation related to the conical die is shown by the chain line in Fig. 16. Likewise as in case (a), the relation of $\bar{\sigma}\sim\bar{\varepsilon}$ was assumed as a straight line. Moreover, $\bar{\sigma}$ was solved with the assumption of pure compression at the extreme periphery.

When $|\sigma_3|$ is determined in accordance with this method of calculation, it will show optimum values whereas, according to the approximate solution method for a flat die under the assumption of an initial value idential to that in (a), $|\sigma_3|$ will show up very small. This phenomenon is caused similarly as noted in (a) to the difference in actual distribution of $\bar{\varepsilon}$ (refer to Fig. 17). σ_1 coincides more closely with the value found by strict calculation as compared to the value derived by the method in (a).

c) *Case according to theory of maximum shear stress (Chapter 1–6)*

The strokes considered in this calculation example are identically the same as in (a) and (b). The assumption is made moreover that the shear stress at the extreme periphery in the case for the flat die as well as the conical die is evenly distributed in the flange. However, it is assumed that the strain in the extreme periphery in the case of the flat die takes place two dimensionally as in (b) whereas, the extreme periphery in the case of the conical die is assumed to be under pure compression.

The calculated solutions respective to the flat die and conical die are indicated by the fine lines in Fig. 15, 16. In the calculation case for the flat die, it will be noted that two fine branches develope from the point of contact to the die shoulder. The lower fine line is the result of calculation with the assumption of flatness of the flange with disregard of the roundness of the die shoulder. The upper line includes the effect of friction at the die shoulder and represents a multiplication of the value given by the lower line by $e^{\mu(\theta-\alpha)}$ by following the procedure used by Sachs.

According to the above treatment of stresses, the drawing force when calculated will be approximately 1,300 kg or about 23.5% lower than the experimental value.

The strain at the point R_4 may be determined from geometrical relations since the factor of thickness variation is neglected. Therefore, if the principal shear stresses found for R_0 and R_4 are averaged and applied on the deformation resistance k, the difference between calculated and experimental values may be further decreased.

If the stress distribution calculated according to a strict solution and the stress distribution determinable by an approximate solution as described above are com-

pared, it will be found that σ_3 will vary widely depending on the method of calculation while the variation of σ_1 would be small.

The above may be interpreted simply as being attributed to the fact that the radial stress component σ_1 is the value of the circumferential stress σ_3 integrated with respect to R. This will moreover mean that there will be no large discrepancy in calculating the drawing force by either of the methods.

For comparative reference, Table 3 gives the comparison of drawing forces calculated in accordance with various methods for the case for deep drawing with a flat die involving a stroke of 17 mm (stroke at maximum drawing force).

TABLE 3. COMPARISON OF PUNCH FORCES CALCULATED BY VARIOUS METHOD AND OBTAINED EXPERIMENTALILY, WHEN STROKE OF DRAWING ON FLAT DIES IS 17 MM (CORRESPONDIG TO MAX. PUNCH FORCE)

Methods of numerical calculation	Punch forces		Differences
	Experimental values kg	Calculated values kg	%
Local variation of thickness and strain hardening are taken into consideration (II-2).	1700	1655	− 3
Local variation of thickness is taken into consideration, while strain hardening are assumed to be constant over flange (II-4).	1700	1391	−18
Strain hardening is assumed to be constant over flange, and thickness is assumed to remain to initial thickness of blank (II-4).	1700	1389	−18
Max. principal shearing stress theory (II-5).			
$k=(\sigma_1-\sigma_3)$	1700	1300	−23.5
$k=1.10(\sigma_1-\sigma_3)$	1700	1430	−16
Experimental formula [8].			
$P_{max}=3(\sigma_b+\sigma_s)(d_0-d_2-r_d)t_0$ kg	1700	1958	+15

It is found that the drawing force calculated according to the maximum shear stress theory is the smallest. However, if the average deformation resistance is taken as $k=1.1(\sigma_1-\sigma_3)$ as did Sachs, the value of the drawing force will approach experimental values to a degree within practical application.

The "experimental formula" noted in the aforenoted table refers to the equation:

$$P_{max}=3(\sigma_b+\sigma_s)(d_0-d_2-r_d)t_0 \quad \text{kg},$$

heretofore introduced by the authors [8] in which, σ_b is tensile strength, σ_s as 0.2% residual strain yield stress, d_0, d_2 and r_d are initial blank diameter, die hole diameter and die shoulder radius respectively and t_0 is the original thickness of the blank.

Referring to the above table, it can be said that precluding the case of calculations by faithful consideration of all factors or by experimental formulae, the drawing force determined by any approximate method of solution would not only be substantially small but also be absent of any marked mutual differences. Although the drawing force determined by experimental formulae is greater, it is from a practical standpoint with permissible limit.

Insofar as the determination of the strain distribution is concerned, it is desirable to calculate this distribution by setting up a true formula as it has been found that a direct relation cannot be tied-in with the most simple shear stress theory and the reason of excessive divergence from actual condition when other approximate calculation methods are employed.

6. *The effects of mechanical properties $\bar{\sigma}\sim\bar{\varepsilon}$ of materials on stress and strain distribution*

When the plastic curve of a material is approximated in accordance with the power law $\bar{\sigma}=K'(\bar{\varepsilon})^n$, the characteristic of work hardening of the material can be judged by the magnitude of the power n. For instance, the power n for material such as duraluminium, aluminium which are comparatively free of work hardening, ranges between 0.1–0.2 and generally between 0.4–0.5 for brass, stainless steel and other. The n for materials commonly used for drawing ranges between 0.1–0.5.

Now an investigation was made as to the effect of different materials on stress distribution and strain distribution by taking three types of materials ($n=0.1$, 0.52 for phosphor bronze subject to test, and 1.0) and by solving in accordance with a strict method of solution (Refer to Fig. 18).

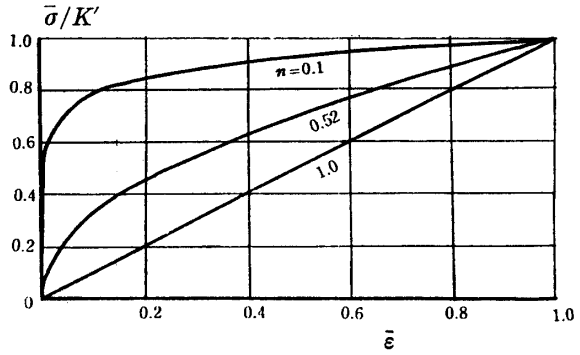

FIGURE 18. Plastic curves with parameter n.

For the purpose of illustration, a stroke of 17 mm for the case of the flat die in (2) will be selected for calculation. In other words, a blank with a radius r_0 approximately twice the diameter r_1 of the punch will be shrunk or drawn until the ratio of the extreme outer circumference R_0 to r_0 reaches about 0.77.

Fig. 19 indicates the stress distribution according to calculations. Although σ_3 displays a tendency to change along the radial direction depending on the magnitude of n, σ_1 on the other hand indicates a steady tendency for reasons as previously denoted.

The strain distributions as determined from the aforesaid stress distribution is shown in Fig. 20 wherein it will be noted that although different materials may be used, the strain distribution in the flange portion as in the portion corresponding to the portion of the die shoulder are practically the same. This can be readily understood if we consider that deep drawing work of a cylinder is controlled by the axis and since the shape is determined by the die, the freedom to affect the state of deformation becomes limited.

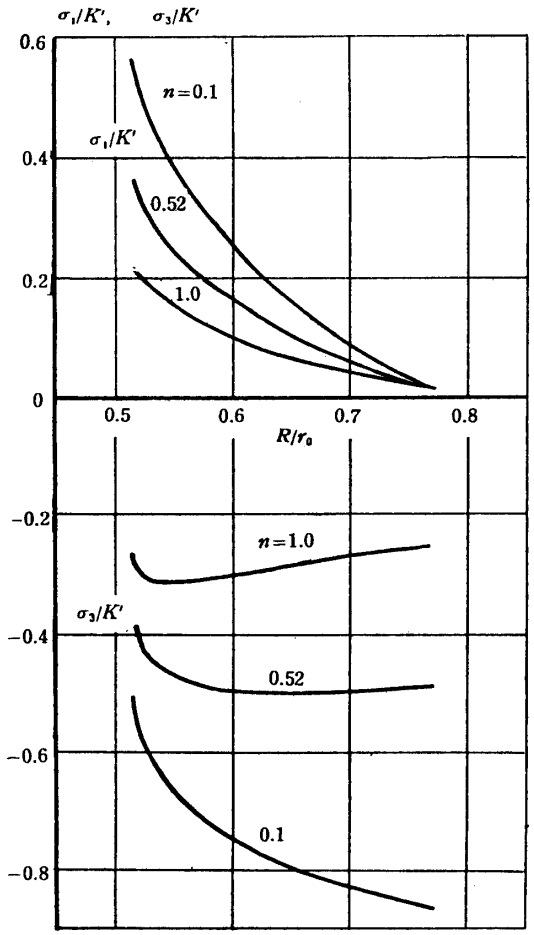

FIGURE 19. Comparison of stress distribution with parameters n over flange part AC, when drawn to a stroke of 17 mm by flat die.

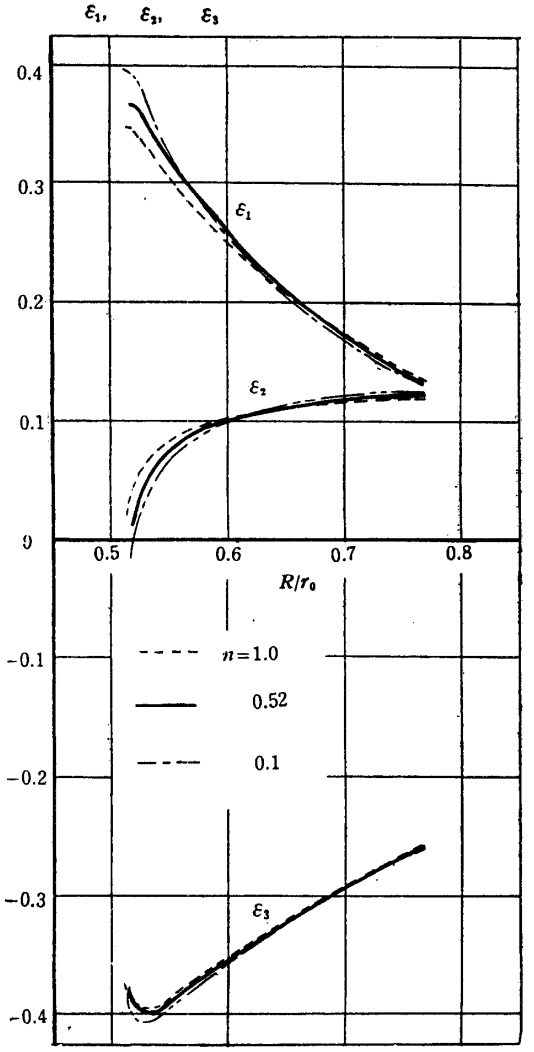

FIGURE 20. Comparison of strain distributions with parameters n over flange part AC, when drawn to a stroke of 19 mm by flat die.

PART III
FORMABILITY TESTS [9]

Testing methods presently employed in judging the formability of materials may be divided into indirect testing comprising such as tensile testing and hardness testing, and direct testing involving actual deep drawing work. Generally, the individual test values obtained from indirect testing have practically incomplete relation to formability and as the method based on direct testing is preferred, several investigations were made in this respect.

1. *The relation of work hardening constant n to formability*

If σ_p and ε_p determinable from tensile tests on a material as described heretofor and their relation approximate according to the equation $\sigma_p = K'\varepsilon_p^n$, the tensile

strength would be expressed as $\sigma_b = K'(n/e)^n$. Moreover, and according to the approximate solution applicable to deep drawing with a conical die as indicated in I–6, the maximum drawing stress $(\sigma_1)_m$ for $R = R_4$ would be solved by the following equation.

$$(\sigma_1)_m = e^{\mu\theta}\left(1+\frac{1}{B}\right)\left\{1-\left(\frac{\zeta}{\eta_m}\right)^B\right\}K'(\ln \eta_m)^n . \tag{28}$$

Now, if we assume that the drawing limit is reached when the maximum drawing stress equals the tensile strength, the drawing limit would be given by following equation.

$$(\sigma_1)_m = K'\left(\frac{n}{e}\right)^n . \tag{29}$$

In the preceding equations, $B = \mu \cot\theta$, $\zeta = R_4/r_0$ and η_m represents the ratio of R_0 to r_0, i.e., (R_0/r_0). Since η_m, as noted hereafter, is a function of n, the drawing limit would be established by given values to n. Therefore, the work hardening constant n can be used as an element in judging the formability of a material.

C. Arbel [*10*] investigated the relation of n to formability experimentally with respect to aluminum, copper, brass and stainless steel and deduced the conclusion that good formability would be obtained as the bigger n becomes.

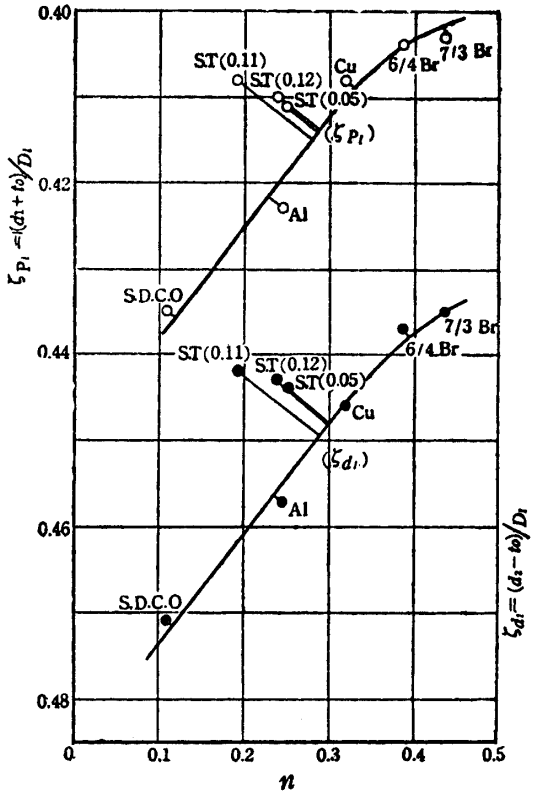

FIGURE 21. Relation of work hardening constant to drawing limit (Experimental result).

Fig. 21 indicates the experimental findings of the authors with the exception of mild steel (S.T.) which indicates a different characteristic, the results respective to

other materials coincide with those obtained by C. Arbel. Consequently, it would be illogical and false to compare the formability of all materials principally on the basis of the magnitude of n. In other words, a cause for this departure may be attributed to the fact that the fracture strength of the blank coming into contact with the corner of the punch head is not equal to the tensile strength and that the formability is not a simple function only of n. Put in other words, the point of fracture is subjected to bending in the initial stage of deep drawing followed by a deformation under multiaxial stresses and is affected by the friction between the blank and punch surface. A simple factor to investigate the influence of these various factors is taken as the ratio of σ_z/σ_b i.e., the maximum punch force P_m in forming a blank with a drawing limit divided by the cross sectional area of drawn shell ($\sigma_z=P_m/\pi(d_1+t_0)t_0$) to σ_b (See Table 4). In view of the differences in magnitude in the ratio of apparent fracture strength σ_z to σ_b and the extremeness with respect to mild steel, we can consider this as good reason to support our viewpoint that the formability of a material cannot be and should not be compared pricipally on the basis of n.

TABLE 4.

Material	Thickness mm	Hardness V. H. N.	Ultimate strength σ_b kg/mm^2	σ_z/σ_b (case of flat die)	n	Limiting drawing coefficient D_l/d_1	Limiting drawing ratio $\zeta_l=D_l/d_4$
AI	1.0	26.0	9.6	0.98	0.246	0.403	2.188
S. D. C. O.	1.0	53.0	18.3	0.92	0.110	0.415	2.124
Cu	1.0	43.2	23.5	1.07	0.341	0.389	2.269
7/3 Brass	1.0	66.4	34.2	1.07	0.439	0.386	2.299
6/4 Brass	1.0	94.7	38.7	—	0.386	0.385	2.290
ST. (0.05)	1.0	94.7	34.3	1.22	0.246	0.392	2.252
ST. (0.11)	1.0	93.6	33.4	1.07	0.194	0.390	2.264
ST. (0.12)	1.0	166.0	37.2	1.12	0.240	0.391	2.256

2. *Formability test with a conical die*

When the ratio of r_0/t_0 ranges approximately between 25–35 in deep drawing work involving a conical die (Fig. 22), a blank holder would not be necessary and the work would be made easy. Moreover, it provides the added feature that the difference in forming limit due to differences in the dimention and shape of the die would not be as pronounced as in the case for a flat die. According, an investigation was made as to the simplication of the direct testing method by deploying these features.

a. *Maximum punch force method*

Although the limit of deep drawing can be found accurately by determining the maximum diameter of a blank drawable from circular blank of various dimensions, this method is time consuming, tedious and impractical.

Now, the relation between the diametrical dimension of a blank and the maximum punch force within a reasonable range will be of linear nature. Moreover, a

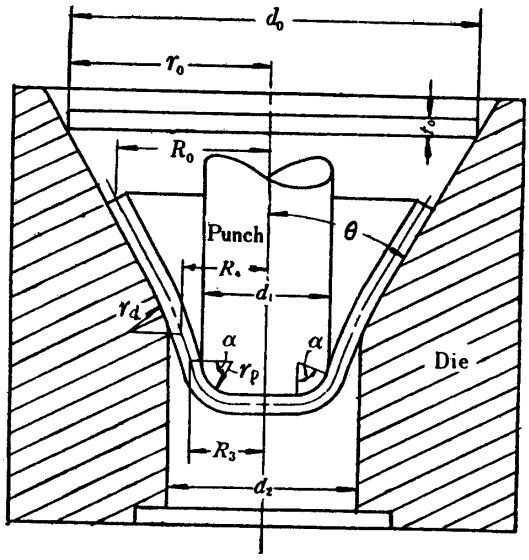

FIGURE 22. Deep-drawing by conical die.

linear relation also exist within a certain range between the fracture force and blank diameter in treating with blanks beyond their drawing limitations. Now, if these relations are plotted as shown in Fig. 23 and deep drawing limit established from the intersection of the straight lines, it may make it possible to reduce the number of necessary blank or from the standpoint of time, derive the limit more quickly.

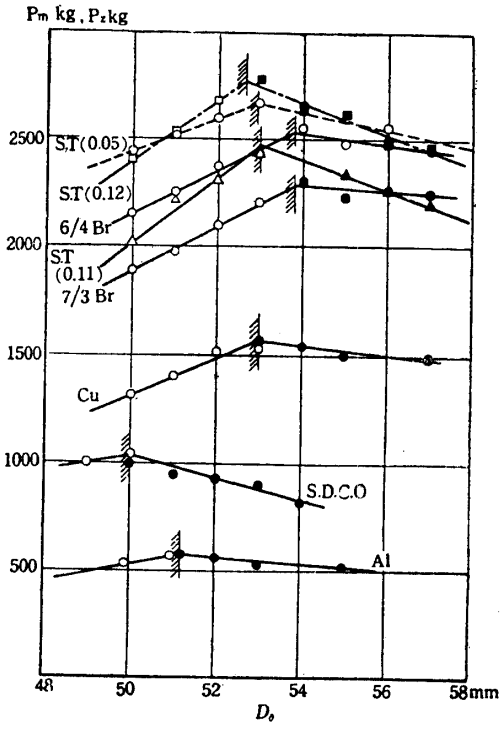

FIGURE 23. Determining the drawing limit by max. punch force method.
▲, ■, ●; Fracture forces at bottom of shell.
△, □, ○; Max. punch forces of deep-drawing.

b. *Diametrical ratio method*

If the friction constant is assumed to remain constant in the course of deep drawing work, the maximum punch force would be reached when the differential equation for σ_1 at $R=R_4$ satisfies

$$\frac{d(\sigma_1)_{R=R_4}}{d\eta}=0\,.$$

Consequently, we have

$$\frac{d}{d\eta}\left[(\ln\eta)^n\left\{1-\left(\frac{\zeta}{\eta}\right)^B\right\}\right]=0\,,$$

$$\therefore\quad \zeta^B-\frac{n\eta_m^B}{n-B\ln\eta_m}=0\,. \tag{30}$$

Wherefrom, we can determine η_m in the case of drawing a blank of ζ.

If the fracture strength equals the tensile strength, we will then have

$$\zeta^B-\eta_m^B\left(1-\frac{A}{(\ln\eta_m)^n}\right)=0\,, \tag{31}$$

when

$$A=\left(\frac{n}{e}\right)^n\left(\frac{B}{1+B}\right)\frac{1}{e^{\mu\theta}}\,.$$

Wherefrom the relation of η_m to ζ would be established.

Now, the relation of the diametrical ratio η_m found accordingly to the formability is identically the same as the relation of n to formability. As noted previously, the effect of the fracture strength must be accounted for in the test values which can be taken care of by working with a plate larger than its drawing limit and by employing the diametrical ratio $R_0/r_0=D_0/d_0$ corresponding to the instant of fracture (Fig. 24).

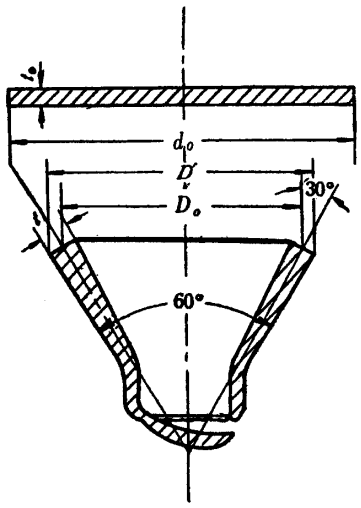

FIGURE 24. Test piece at the instant of fracture at the shell bottom.

Fig. 25 shows the results found experimentally on the relation of the diametrical ratio $\eta_{(\xi=1.4)}$ corresponding to the instant of fracture at the shell bottom to the deep drawing limit respective to a blank 1.4 times the punch diameter. According to this method, the maldistribution as was found to be associated with mild steels in Fig. 21 now coincides with the lines of other metals wherefrom it can be seen

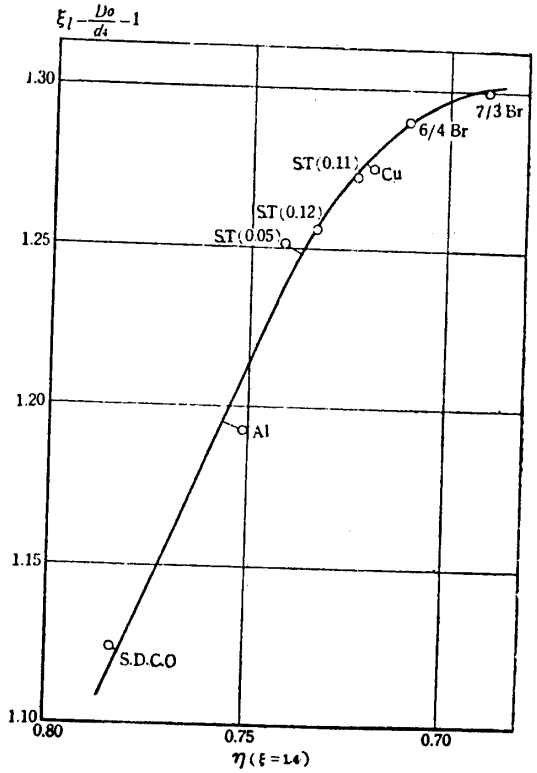

FIGURE 25. Relation of diametrical ratio to drawing limit (Experimental results).

that the comparison of formability can be accurately on the basis of the diametrical ratio. According to this method moreover, it would only be necessary to employ blanks of one diameter, introduce great savings in testing time and incidental expenses and serve sufficiently for practical testing applications in the plant.

In conjunction with the employment of this diametrical ratio method for material selection purposes, it has the shortcomings of insufficient contribution of the fracture strength to the test values due to the occurence of fractures at a shallow drawing depth and in producing wrinkless if the diameter of the blank used is too large. Consequently, it is preferable to use blank of a diameter just as small as is allowable and when established according to the formula $d_0=(2.6\sim3.0)d_1$, it would prove satisfactory.

In actual working conditions, combinations of deep drawing and bulging or stretching are oftentimes encountered, under these circumstances, the use of a spherical punch head is believed to be suitable in selecting materials properly. It is understood of course that it is preferable to employ a flat nosed punch for pure deep drawing work.

Summary

This analysis for deep drawing of cylindrical shells was made on the basis of the total strain theory and octagonal shear-strain relation with due consideration of the differences in local work hardening, thickness variation and by thorough analyses of actual drawing phenomena. The analysis also undertook to approximate the equivalent stress $\bar{\sigma}$ and equivalent strain $\bar{\varepsilon}$ according to the power law.

Actual experiments were also performed by using a flat die and a conical die for deep drawing of phosphor bronze plates with the least directional deficiencies in verifying the results of calculations.

It was found that the drawing force as well as the strain distribution according to calculations coincided very closely with experimental findings. Furthermore, the results of this experiment was checked compared against those derived from miscellaneous approximation methods heretofore published. Moreover, it was verified that there is practically no difference in the strain distribution in the flange and the portion in contact with the die shoulder during the course of drawing irrespective of the material used.

Furthermore and according to results of investigations related to formability testing, it has been confirmed than the magnitude of the flange diameter produced at the point of fracture of a blank greater than its drawing limit and formed with a conical die, can properly used in comparing the formability qualities of materials.

In closing, the authors wish to express his deep appreciation to Messrs H. Kudo, S. Fukuda, T. Hojo, H. Okawa, K. Abe for the assistance and help lent in carrying out and conducting calculations and experiments. The authors moreover wishes to note that a subsidy was received in the early stage of this research program for scientific research funds from the Ministry of Education.

Department of Materials
Aeronautical Research Institute
University of Tokyo, Tokyo
May 21, 1958

References

[1] M. Sommer; Forsch-Arb. V. D. I. Ht. 286, (1926).
[2] G. Sachs; Mitt. D. Mat.-Pruf.-Anst.-Sonderht, 16, (1931), P. 11–38.
[3] M. Masuda; Trans. Japan Soc. Mech. Engrs. Vol. 8 (1942), Vol. 11 (1945), Vol. 18 (1952).
[4] S. Fukui; Sci. Pap. I. P. C. R. Vol. 34 (1938), P. 1422–1527, Vol. 35 (1939), P. 377–385.
[5] S. Fukui, H. Yuri and K. Yoshida; Rept. Inst. Sci. Tech., Univ. of Tokyo, Vol. 8 (1954), P. 179–196.
[6] M. H. Lee Wu; N. A. C. A. Report, 1021 (1951), P. 1–23.
[7] R. Hill; The Mathematical Theory of Plasticty, (1950), P. 278–283.
[8] S. Fukui, K. Yoshida and K. Abe; Rept. Inst. Sci. Tech., Univ. of Tokyo, Vol. 8, (1954), P. 23–30.
[9] S. Fukui, H. Kudo, K. Yoshida and H. Okawa; Rept. Inst. Sci. Tech., Univ. of Tokyo, Vol. 6 (1952), P. 351–357.
[10] C. Arbel; Sheet Metal Indust., Dec., (1950), P. 926.